JOURNAL OF GUIDANCE, CONTROL, AND DYNAMICS
Vol. 19, No. 5, September–October 1996

Development and Flight Testing of Quantitative Feedback Theory Pitch Rate Stability Augmentation System

Paul L. Fontenrose* and Charles E. Hall Jr.†
North Carolina State University, Raleigh, North Carolina 27695-7910

The design of a quantitative feedback theory control system to improve the flight handling qualities of an unmanned aerial vehicle (UAV) at relaxed stabilities is illustrated. Aircraft flown at low static margins are significantly more efficient than conventional designs, but without stability augmentation they are difficult if not impossible to control. Longitudinal stability augmentation is achieved by using an onboard computer system to calculate control surface deflection based on the sensed pitch rate of the aircraft and pilot elevator commands. The quantitative feedback theory controller was implemented on this computer system to provide acceptable handling characteristics for a large portion of the UAV's flight envelope. The flight tests of the UAV, which resulted in the successful completion of an entire flight at a 2.5% static margin, are also described.

Introduction

A SIGNIFICANT amount of research effort is spent by controls engineers today in the development of control systems that are robust to plant variations and parametric uncertainty. These robust control techniques have a particularly useful application in the design of aircraft control systems. This is because aircraft dynamics vary substantially throughout the flight envelope. Variables such as airspeed, fuel consumption, and the amount and location of payload can have a dramatic effect on the aircraft's plant parameters. One method of designing robust control systems is through the use of quantitative feedback theory (QFT). QFT was invented by Issac M. Horowitz in the early 1970s and has experienced a rigorous developmental period over the past two decades.[1–7] During this developmental period, a large number of papers have been written detailing designs using the QFT technique. A few examples of these designs are detailed in Refs. 8–10. Not until the last 10 years, however, has the application of QFT in flight control system designs been studied extensively.[11,12] The cornerstone of this flight control research was focused in the Flight Dynamics Laboratories at Wright–Patterson Air Force Base in Dayton, Ohio. The research at these labs culminated in the design and first successful flight testing of a QFT flight control system.[13] These flight tests, completed in 1992, have remained the only QFT flight tests up to the date of this research. Based on these results, the goal of this research was to continue the recent development of the study of QFT in flight control applications and to perform an independent study of QFT at North Carolina State University (NCSU).[14] This goal led to an extensive list of objectives. The first of these objectives is the investigation of the QFT design technique itself. This includes its application to continuous and discrete time systems and the practical implementation of QFT on such systems. In addition to studying the technique, the research also contains the design and programming of any computer codes or programs necessary for both the development of the QFT control law and for the hardware implementation of the QFT control structure. This includes the development of a computer-aided design (CAD) package to facilitate the design of future QFT control systems and the programming of flight computer codes for a NCSU flight computer system (FCS). Only after the design of this infrastructure to develop and implement the QFT control system could the main objective of this research be realized. The objective is the development of a flight control system for an existing NCSU unmanned research vehicle. This vehicle is equipped with a variable center of gravity (c.g.) mechanism that enables the static margin of the vehicle to be varied during flight. This control system design is to exhibit robustness for the vehicle's varying static margin range and for a defined velocity range. Finally, the last objective is the execution of a series of flight tests to fully analyze the performance of the QFT control system and its ability to meet specified performance requirements over the defined flight envelope.

Received Oct. 31, 1995; revision received April 30, 1996; accepted for publication May 4, 1996.

*Graduate Student, Department of Mechanical and Aerospace Engineering, P.O. Box 7910. Member AIAA.
†Assistant Professor, Department of Mechanical and Aerospace Engineering, P.O. Box 7910. Member AIAA.

QFT Design on a Variable c.g. Aircraft

The object of the single input/single output (SISO) QFT design technique is to design a prefilter F and a compensator G for the QFT feedback structure shown in Fig. 1. Because this system actually consists of two disturbance inputs (D_1 and D_2) and one commanded input (R), it is sometimes refered to as a multi-input/single output (MISO) system.[6] This feedback structure also contains an output Y and the system plant P. Because there are three inputs in this feedback structure, three input–output relations can be developed. These are

$$T_{D_1} = Y/D_1 \tag{1}$$

$$T_{D_2} = Y/D_2 \tag{2}$$

$$T_R = Y/R \tag{3}$$

Equations (1) and (2) are disturbance relations and Eq. (3) is the traditional SISO commanded input–output relation. The compensator G is required to ensure that the disturbance rejection input–output relations T_{D_1} and T_{D_2} fall within the set of acceptable disturbance input–output relations, defined early on in the design process. This set of input–output relations is called a disturbance rejection thumbprint when it is graphically displayed on a Bode plot. Both the compensator and the prefilter F are required to ensure that the tracking input–output relation T_R falls with the set of acceptable tracking input–output relations (i.e., the tracking thumbprint). All of these relations must be satisfied for the entire plant uncertainty range. This plant uncertainty range is quantitatively defined by creating a

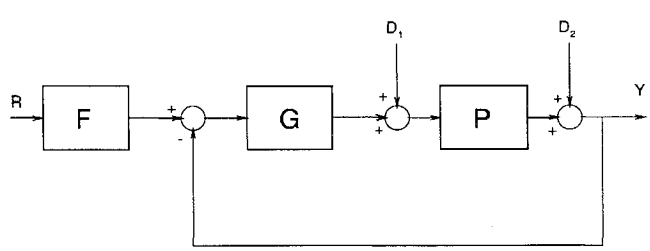

Fig. 1 QFT feedback structure.

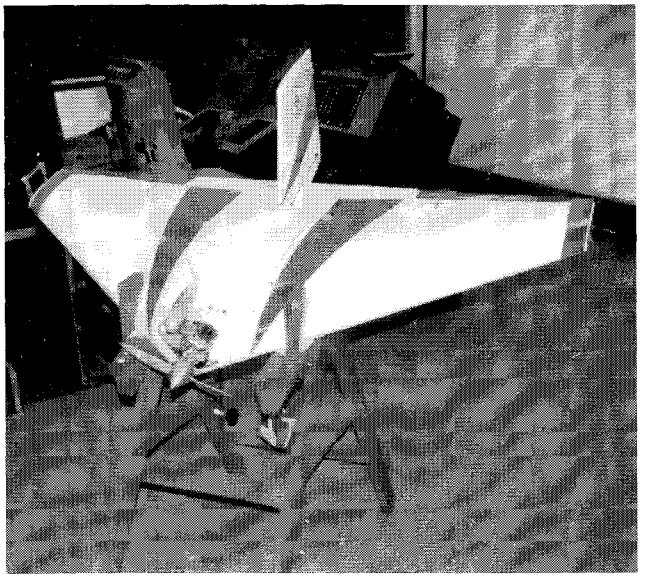

Fig. 2 Photograph of UAV.

set of distinct plants that represent the parameter uncertainly and variation in the actual plant, which in this case is the longitudinal dynamics of the aircraft plant.

The application of this technique for the design detailed here involves a controller design for a stability augmentation system (SAS) that will provide controllable flight at a range of reduced static margins for a large portion of the flight envelope. To accomplish this, the QFT design was performed for a quantified parameter uncertainty range that included static margin and flight velocity. This design was performed utilizing only pitch rate feedback and pilot elevator input.

Flight Vehicle Description

The vehicle used in this design was a prototype tailless cropped delta-wing unmanned aerial vehicle (UAV) (Fig. 2), which was built at NCSU in 1992.[15] The vehicle is constructed of a fiberglass composite and weighs approximately 21.0 lb. This vehicle is equipped with a throttle and three control surfaces. The control surfaces are left and right elevons and a rudder. The power plant is a 10.0-cc two-cycle aircraft engine, which is used in a tractor configuration. To reduce the drag and weight of the vehicle, the aircraft is not equipped with conventional landing gear. A catapult system is used for launching the aircraft, and landing skids are used during recovery. These are mounted to the internal structure on the underside of the configuration. The vehicle has enough volume to carry a number of components. One of these components is a variable c.g. mechanism. This mechanism gives the UAV the capability to change its static margin during flight. The mechanism is composed of two tubes that run longitudinally through the aircraft. Each tube contains a lead slug that is moved with a system of electric motors and pulleys. A servoactuator connected to an auxiliary channel of the radio receiver activates a switch that engages the motors in either direction. Electric sensors in the tube stop the slugs when they get to the correct position. This system allows the static margin to be changed by approximately 8%. In addition to the c.g. mechanism, the aircraft also houses a flight computer system and a flight data recorder. This equipment implements the control law and records hours of flight data. The data retrieved during flight consist of the pitch rate, velocity, engine revolutions per minute, pilot elevon inputs, and the actual elevon deflections.

QFT CAD Package

As a means of facilitating the flight controller design process and also to gain a thorough understanding of the QFT technique itself, a QFT CAD package was designed in conjunction with this research. This package was necessary to shorten the traditionally time-consuming and laborious QFT technique. The CAD package used for this QFT design was designed and programmed using Mathworks™ MATLAB™ software.[16] This package, which consists of approximately 40 MATLAB codes called ".m" files, can be used to design MISO QFT controllers using both the pseudocontinuous time (PCT)[6] and the w-domain[6] design methods.

Model Development

The first step to an accurate controller design is to develop an accurate model of the system. To simplify the QFT design process, instead of developing a traditional four-state representation of the aircraft dynamics (which contains both the short period and phugoid modes of the aircraft), a second-order short period approximation was used to represent the aircraft for the control system design. This can be done because the focus of the design is on improving the short period response of the aircraft and not the slower phugoid response. This short period approximation contains only the angle of attack and pitch rate state variables. It should be noted, however, that the traditional fourth-order representation of the system was used for simulation of the controller performance. For both representations, the nondimensional aerodynamic coefficients for the aircraft were computed using a potential theory paneling code called PMARC.[17] The input for both of these systems is the actual elevator deflection δ_e, and the output is the pitch rate of the vehicle q.

In addition to representing the longitudinal dynamics of the aircraft, the elevator servo is also modeled. The commanded elevator from the pilot or the control system, denoted δ_{e_c}, is transferred to the surface through this servoactuator. A model of this actuator must be included in the overall system representation. The servoactuator used on the aircraft elevators is a commercially available JR 4031 electrical servo and is best represented by a second-order model. The transfer function for this model is

$$\frac{\delta_e}{\delta_{e_c}} = \frac{\omega_{n_{\text{SERVO}}}^2}{s^2 + 2\zeta\omega_{n_{\text{SERVO}}}s + \omega_{n_{\text{SERVO}}}^2} \tag{4}$$

where $\omega_{n_{\text{SERVO}}}$ is the natural frequency of the servo and ζ is the damping ratio of the servo. It can be seen that the commanded elevator position is the input of this transfer function, and the actual elevator position is the output. The damping ratio and natural frequency of this servo were experimentally determined.[18] The results from this process showed that the servo's damping ratio was 0.65 and its natural frequency was 30 rad/s with no loading on the servo. Although the servodynamics could be affected by loading on the control surfaces during flight, this effect was considered minimal because of the tremendous power of the JR 4031 servo compared with the aerodynamic forces that the surfaces experienced. The addition of the servomodel increases the order of the short period approximation system from two to four. The input of this system is the commanded elevator deflection, and the output is still the pitch rate.

QFT Design for a Pitch Rate SAS

As was mentioned previously, the goal of the QFT technique is to design a compensator G and a prefilter F for the QFT system shown in Fig. 1. Notice that, for a pitch rate output, the QFT system requires a pitch rate input from the pilot. Traditionally for longitudinal control systems, the pilot commands an elevator deflection and not a pitch rate. Fortunately, this situation is easily remedied. In the linear region of the flight regime, the pitch rate of an aircraft is essentially proportional to elevator deflection. Therefore, a gain can be applied to the pilot's elevator command to transform the elevator commanded into a commanded pitch rate. The gain is labeled K_{pilot}. During the flight test of another control system at a 5% static margin,[19] the pilot felt comfortable with the performance of the vehicle when the aircraft's pitch rate was four times the elevator deflection angle. Based on this previous test, a K_{pilot} of 4 (/s) was selected.

Plant Set Selection

The first step to a QFT design is to select a set of plants that represent the entire range of parameter uncertainty. The set of plants developed for this configuration is shown in Table 1.

This set represents a parameter uncertainty range of four different parameters. It was originally decided that the main objectives of this design would be a control system for a static margin range of 2.5 to 7.5% and a velocity range of 80 to 140 ft/s. In addition to

Table 1 Aircraft plants

Plant no.	Static margin,%	Velocity, ft/s	Elevator effectiveness	I_{yy}, slug-ft^2	ζ_{SP}	$\omega_{n_{SP}}$, rad/s
1	7.5	140	Full	0.33	0.424	17.42
2	7.5	140	3/4	0.33	0.424	17.42
3	7.5	80	Full	0.33	0.424	9.95
4	7.5	80	3/4	0.33	0.424	9.96
5	2.5	140	Full	0.33	0.582	11.12
6	2.5	140	3/4	0.33	0.582	11.12
7	2.5	80	Full	0.33	0.582	6.36
8	2.5	80	3/4	0.33	0.582	6.36
9	2.5	140	Full	0.30	0.579	11.76

these parameters, the control system was also designed for ranges of elevator effectiveness and moment of inertia about the y axis. It was deemed necessary to design the control system for a range of elevator effectiveness because it was learned that the PMARC paneling code often overestimates the control power of control surfaces. Therefore, the control system was designed for control surface power between the amount predicted by PMARC and 75% of that amount. The moment of inertia was varied with the anticipation that some of the nose ballast would be removed when the aircraft c.g. was changed from 7.5 to 2.5%. Initially, as a safety precaution, the c.g. range was set up only to change from 7.5 to 5.0% during flight. Because of limitations in the possible weight locations of the lead ballast in the c.g. mechanism, additional nose ballast was needed for these flights.

PCT Representation of Plant

The discrete QFT controller design was designed using a PCT technique. This enables the designer to use continuous QFT design techniques during the controller design process. When a PCT approach is used to design a discrete controller, the zero-order hold and the sampler of the system must be represented with a continuous function. To ensure that this representation was accurate, a second-order Padé approximation was utilized for the zero-order hold. The equation of this approximation for the 22.9-Hz sampling rate of the FCS is

$$G_{\text{pa}} = \frac{0.5228}{0.0018s^2 + 0.2612s + 12} \tag{5}$$

The sampler is approximated by the following function:

$$G_{\text{sampler}} = 1/T \tag{6}$$

where T is the 0.04354-s sampling period of the system. Both of these equations were combined and added to the existing model of the plant. A continuous time QFT design could then be performed. The overall representation for the aircraft system was therefore sixth order.

Tracking Requirements

The thumbprint for the selected tracking requirements is shown in Fig. 3. The upper bound of the tracking requirements was designed to have a peak overshoot of 1.5, a settling time of 0.5 s, and a damping ratio of 0.35. The transfer function for this bound is

$$T_{R_U} = \frac{12s + 144}{s^2 + 8.4s + 144} \tag{7}$$

The extra zero in the numerator of this transfer function is included to ensure that the thumbprint widens as the frequency increases. This simplifies the QFT design process.[1]

The lower bound was designed to yield a slightly underdamped response with a damping ratio of 0.95. The transfer function for the lower bound is

$$T_{R_L} = \frac{90}{(s + 10)(s^2 + 5.7s + 9)} \tag{8}$$

The additional pole in this function serves the same purpose as the extra zero in the upper bound. The step response of these functions is shown in Fig. 4. These functions were designed to provide level one flying qualities according to the MIL-F-8785 military specification

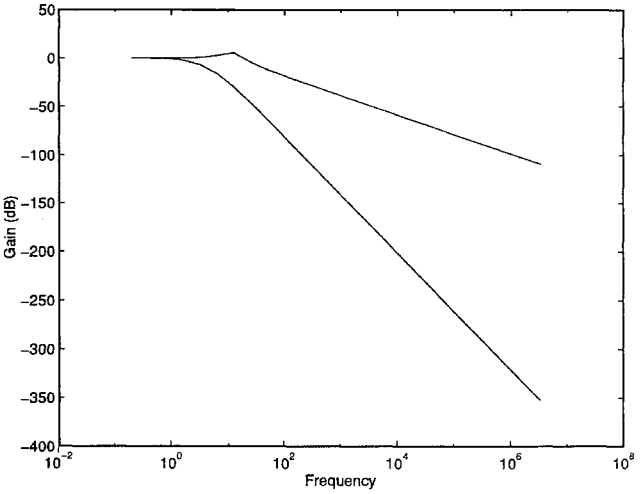

Fig. 3 Tracking thumbprint.

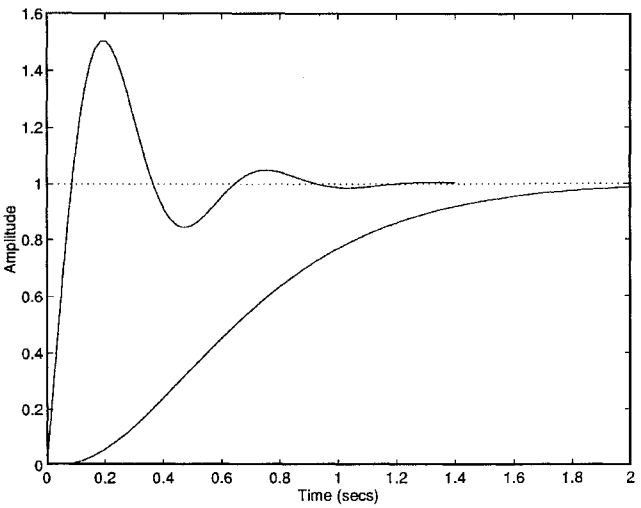

Fig. 4 Step response of tracking requirements.

for fixed wing aircraft. The acceleration sensitivity value (i.e., n/α) used for this determination varied between 10.35 and 31.7 g/rad depending on which plant was used.[20] Although the relevance of this military specification as applied to UAVs is questionable, this served as a general guideline and an adequate starting point for the controller design.

D_1 Disturbance Rejection Requirements

The transfer function that was created as a bound on the D_1 disturbance rejection requirements is

$$T_{D_1} = \frac{s(s + 1)(s + 8)}{(s + 0.5)(s^2 + 1.6s + 4)} \tag{9}$$

The step response for this function is shown in Fig. 5. Note that this step response is fairly relaxed (i.e., $M_p \cong 3$ and $t_s \cong 4$ s). Originally, the requirements on this disturbance rejection case were defined to be much stricter, but because of limitation in the maximum order of the compensator (which is a result of FCS limitations), this bound was relaxed to the function in Eq. (9).

D_2 Disturbance Rejection Requirements

An overdamped response was selected for the D_2 disturbance rejection. The transfer function for this bound is

$$T_{D_2} = \frac{s}{s + 2.3026} \tag{10}$$

This response has a settling time of 1.0 s.

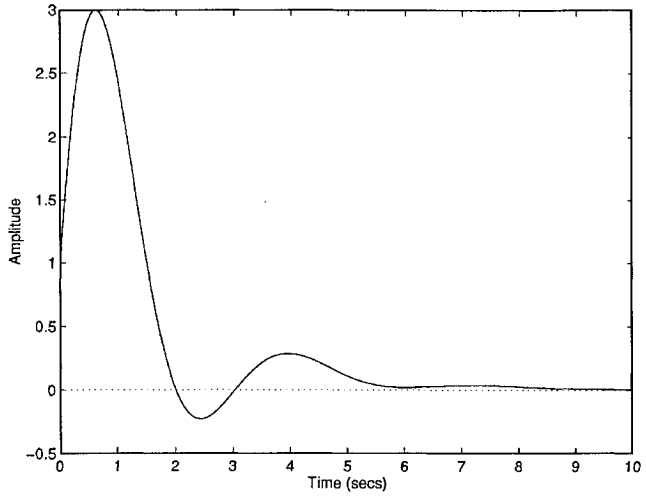

Fig. 5 Step response of D_1 disturbance rejection bound.

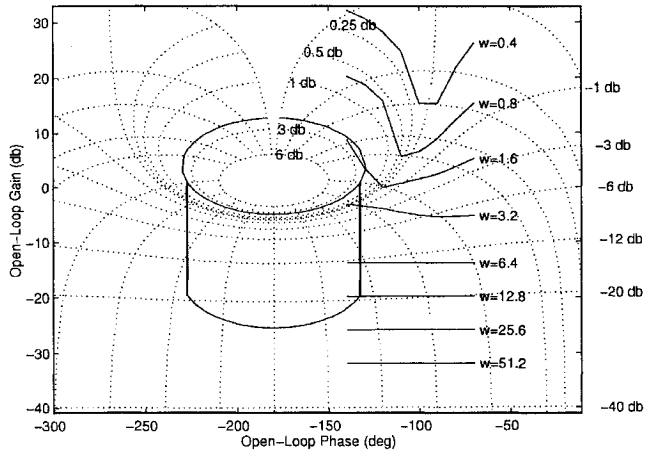

Fig. 6 Optimal bounds [w = frequency (rad/s)].

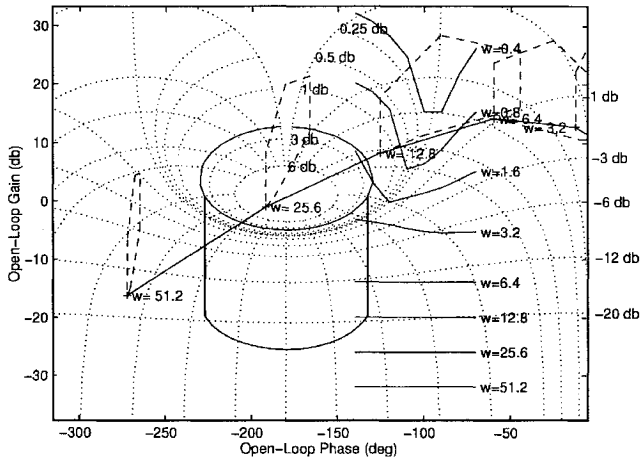

Fig. 7 Loop transmission with $G = 1$ [w = frequency (rad/s)].

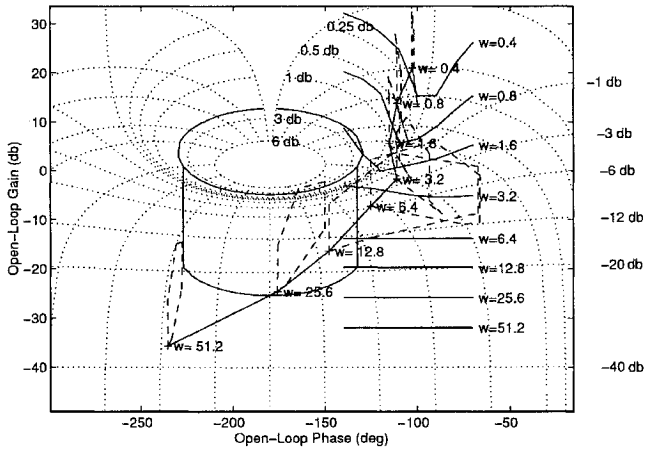

Fig. 8 Loop transmission with $G = 1$ [w = frequency (rad/s)].

U-Contour

The U-contour for this design is shown on Nichol's chart in Fig. 6. The M_L boundary, which is the oval in the center of the Nichol's chart, has a value of 1.5 dB. This corresponds to the minimum damping ratio of the system, which is 0.35. The distance the universal high-frequency boundary is offset (i.e., V) is 20 dB.[6]

Optimal Bounds

The optimal bounds for this design are shown in Fig. 6. These bounds are a composite of the most restrictive cases computed using the previously defined tracking and disturbance rejection performance requirements. The loop transmission on the system must be shaped to adhere to these bounds to guarantee that these performance requirements are met.

Shaping the Loop Transmission

After all of the bounds were determined, the next step was to design the compensator of the QFT system, G, by shaping the loop transmission (which is defined as $L \equiv GP_0$, where P_0 is an arbitrary plant from Table 1). The loop transmission for a compensator value of unity [i.e., $G(s) = 1$] is shown in Fig. 7 along with the optimal bounds, plant templates, and U-contour.

It can be seen in this plot that the bounds are clearly violated at many different frequencies. After the trial and error method of shaping the loop transmission, the loop transmission as shown in Fig. 8 was selected. It can be seen that all of the optimal bounds are satisfied, and the M_L contour is also satisfied for all frequencies except for 25.6 rad/s. At this frequency the template slightly enters the M_L contour. The effect of this on the system is that the plants in the thin strip of the template that enters the M_L contour will have a damping ratio slightly less than the 0.35 value that corresponds to the contour. This violation was deemed acceptable. Also notice that it appears that the high-frequency portion of the U-contour is violated at a frequency of 12.8 rad/s. But recall that the only purpose of the U-contour is to ensure that the plant templates remain outside of the M_L contour. And, as it has already been stated, this template does in fact satisfy the M_L contour. Therefore the U-contour is not an accurate bound at this frequency. The continuous transfer function for this compensator is

$$G(s) = \frac{1.5[(1/4)s + 1][(1/11)s + 1][(1/18)s + 1]}{s(s + 1)\{(1/200^2)s^2 + [2(0.6)/200]s + 1\}} \tag{11}$$

Prefilter Design

The design of the compensator only guarantees that the disturbance rejection requirements will be met and that the magnitude range of the template at each frequency will correspond to the tracking thumbprint. To ensure that the tracking requirements will be met, a prefilter was designed. The frequency response of the final prefilter design is compared with the upper and lower frequency bounds in Fig. 9. Notice that the bounds are met at all frequencies except for between 0.8 and 2 rad/s. At these frequencies the prefilter transfer function F slightly fails the bounds. This was deemed acceptable, after it was determined that the cost of alleviating this situation would be much too high. The order of the prefilter is limited to approximately fourth order by the FCS. It would take a much higher order prefilter to adhere to the bounds for the entire frequency range. The consequences of this slight violation of the bounds was investigated through the use of the simulation, and the conclusion was made that its effect was minimal. Also note that the prefilter transfer function fails the bounds above 100 rad/s. This is acceptable, however,

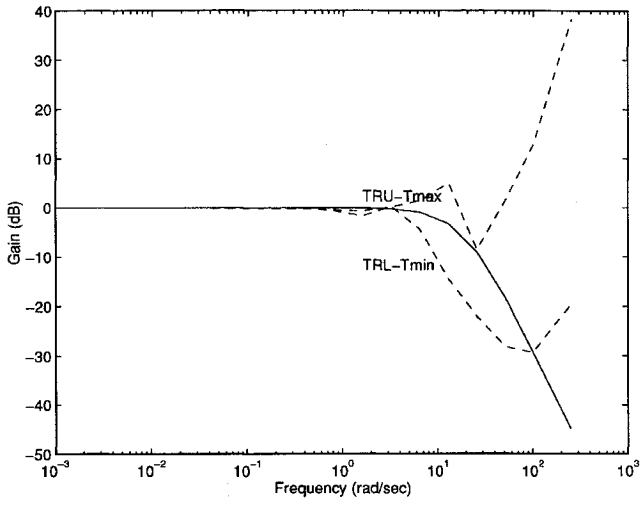

Fig. 9 Prefilter design.

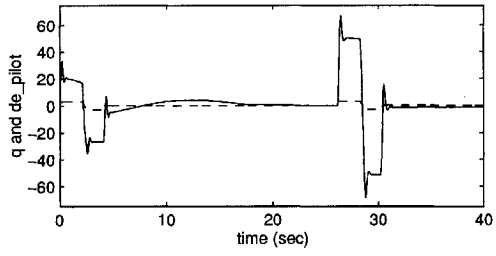

a) Pitch rate output and pilot elevator input (without compensation)

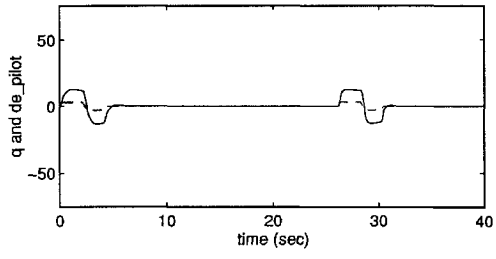

b) Pitch rate output and pilot elevator input (with compensation)

Fig. 10 Simulated elevator doublet responses (with and without control system): ——, q (deg/s) and – –, de_pilot (deg).

because 100 rad/s is well above any frequencies for which the system will be exposed. The transfer function for this prefilter is

$$F(s) = \frac{1}{[(s/18) + 1][(s/20) + 1]} \tag{12}$$

Conversion to Discrete System

The last step required to complete the PCT QFT control system design is to transform the continuous compensator and prefilter into a discrete system via the Tustin transformation.[6,20] Before these controllers were flown, the warping that can occur as a result of the Tustin transformation was investigated as was determined to be acceptable.

Simulation

Before flying the designed control system, it was necessary to verify the controller performance through the use of the simulation provided in the QFT CAD package. This simulation simulated the discrete system exactly as it will be implemented on board the flight vehicle. The only significant difference between the simulation and the actual system is that the actual aircraft dynamics are represented with a fourth-order linear time-invariant state-space model. The simulation uses an in-house servomodel that models both the linear and nonlinear characteristics of the servos used on the aircraft.[18]

Figure 10 shows the simulated response of the aircraft to a set of 3-deg elevator doublets with and without the control system engaged. Between the doublets a simulated c.g. shift from 7.5 to 2.5% static margin occurs. In the uncontrolled case, it can be seen that the magnitudes of the pitch rate response to the elevator doublets vary greatly with static margin. This is not the case with the controlled case; for both static margins the magnitude of the pitch rate is exactly four times the elevator deflection. This is the exact value of the K_{pilot} gain on the control system.

Flight Test Procedure

As was mentioned previously, the delta-wing aircraft used in conjunction with this research was equipped with an FCS, a pitch-rate transducer, an airspeed transducer, and a c.g. shifting mechanism. These components were required to implement the control law, verify the flight envelope of the aircraft, and collect data.

To use these components, a specific in-flight procedure was used. The standard flight procedure began with a takeoff at a 7.5% static margin. During the takeoff the FCS was set in an idle mode. Once airborne, the pilot trimmed the aircraft and then engaged the FCS for the first time. This put the FCS in flight data recorder (FDR) mode. In this mode, the FCS first recorded the trimmed elevator positions and then recorded flight data without implementing the QFT control law. The recorded trim positions were used as zero points for the flight data set. After recording a set of unaugmented maneuvers, the FCS was put back into idle mode. After switching out of the record only mode, the pilot prepared for flight with the control system. The control system was activated every time the FCS was engaged after the initial engagement. This mode of the FCS was denoted the SAS mode. While in SAS mode, a series of maneuvers and/or c.g. shifts were performed. After these were completed, the pilot commanded the lead weights of the c.g. mechanism forward (if necessary) and disengaged the FCS. The aircraft was then landed at this stable unaugmented configuration. This procedure was followed until the final two flight tests. The robustness of the control system was tested more completely during the last two flights by first turning on the control system with the plane untrimmed (to look for the autotrim capability of the control system) and then flying the control system from takeoff to landing at reduced stability with the control system engaged.

Flight Test Results

C.G. Shift Results

The aircraft displayed no c.g. shift induced pitch rate during the transition between any of the vehicle static margins. Flight data taken with the c.g. shifted from 7.5 to 5% are shown in Fig. 11. It can be seen that during the c.g. shift (which was initiated at an FDR time of 79 s), the pilot's elevator commands are essentially zero, whereas the control systems elevator command automatically compensates for the static margin change. Also, after the c.g. shift, the pilot felt no difference in response or handling qualities compared with those of the more stable configuration. These same results were seen when the c.g. was shifted from 7.5 to 2.5%. The only difference between

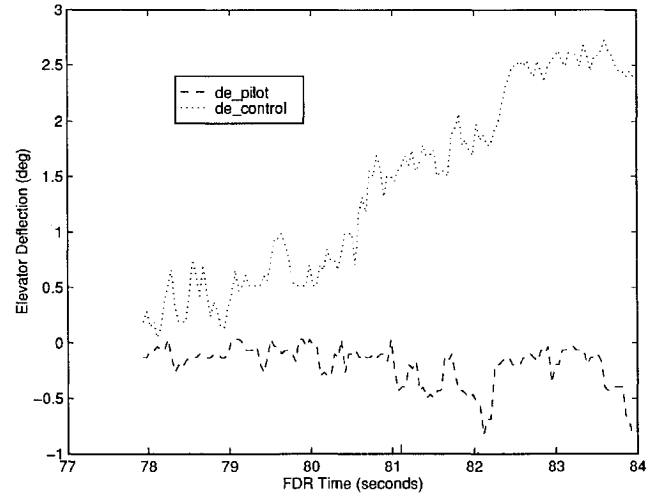

Fig. 11 Elevator deflection during c.g. shift (7.5–5.0%).

c.g. shift data was that, as expected, the elevator deflection change was greater for the 2.5% case. Figure 12 shows the results of this c.g. shift initiated at an FDR time of 52 s. In this case, the change in elevator trim was approximately 5 to 6 deg as compared with 3 deg for the 5.0% static margin case.

Elevator Doublet Results

The elevator doublet data proved to be a very important part of the flight test program. It verified that the control system was working as designed, and it provided a good set of input output data for numerical analysis. The most important result from these doublets is the difference in magnitudes between the controller commanded elevator deflection and the pilots commanded elevator deflections at each static margin. Notice, in Fig. 13, that at a static margin of 7.5% the elevator commands from the controller are greater than those of the pilot. This is not the case when the c.g. is at 5.0%. Here the control systems commanded elevator is approximately the same as the pilot input (Fig. 14). This is because the gain on the pilot input, K_{pilot}, was designed based on 5.0% data from flight data retrieved from previous flight tests of the same vehicle and is a good indication that the control system is compensating for the new stability of the aircraft. At a 2.5% static margin, it was expected that the control system commanded elevator angle would continue to follow the same trend and be less than the pilot commanded input. This can be seen in the plot of the flight data during a elevator doublet at 2.5% (Fig. 15). This plot clearly shows that the elevator deflections commanded by the control system are less than the pilot input commands. This is further evidence that the control system is compensating for the static margin changes.

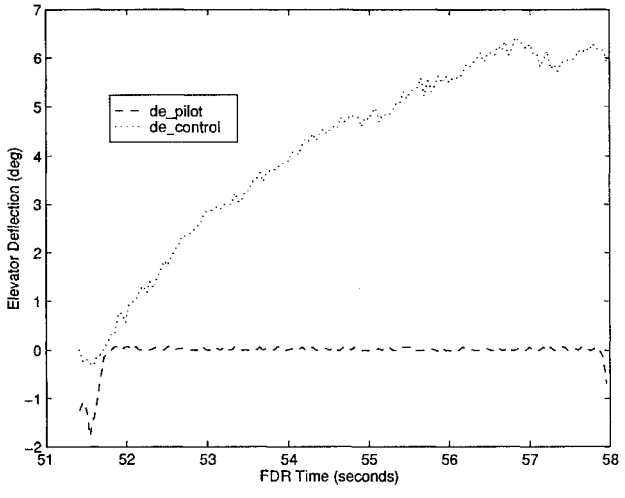

Fig. 12 Elevator deflection during c.g. shift (7.5–2.5%).

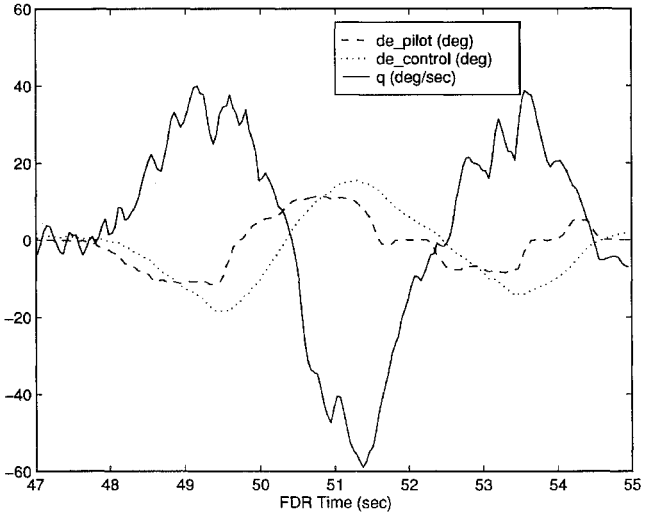

Fig. 13 7.5% static margin elevator doublet.

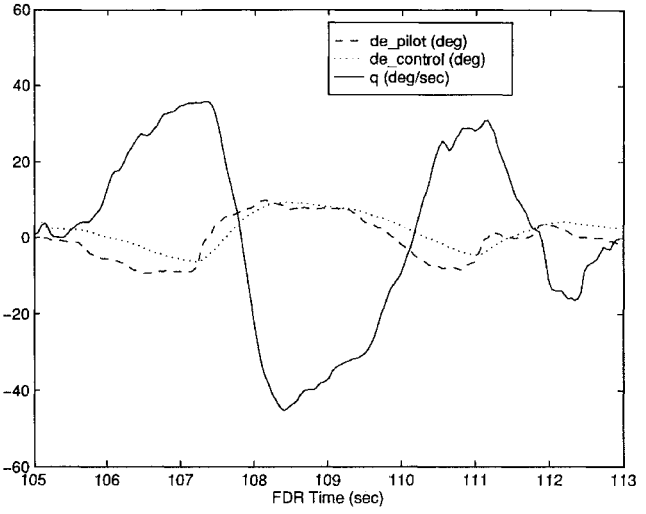

Fig. 14 5.0% static margin elevator doublet.

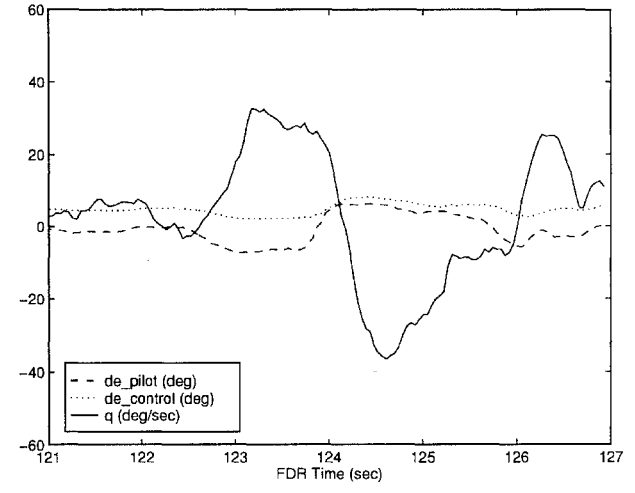

Fig. 15 2.5% static margin elevator doublet.

Autotrim Test Results

The autotrim test was extremely successful. The control system automatically adjusted the elevator deflection to damp the vehicle's initial pitch rate and continued to trim the vehicle throughout the remainder of the flight. It took the control system less than 1 s to damp the pitch rate after the control system was engaged. It should be noted that this autotrim capability of the control system is a result of the free integrators in the loop transmission transfer function. The existence of at least one free integrator is guaranteed by the QFT design process.

Complete Flight Test Results

The final flight test to date of the QFT SAS consisted of an entire flight (i.e., from takeoff through landing) with the control system engaged. This was accomplished at the reduced static margin value of 2.5%. The plane responded extremely well throughout the test and the flight data showed improved performance over the entire flight envelope, including a dramatic improvement in takeoff performance as a result of the reduction in trim drag associated with the reduced static margin.

Numerical Evaluation of Flight Test Results

In addition to the results presented earlier, it is also desirable to numerically determine how well QFT worked in the design of the control system. One way to accomplish this is to try to identify the short period modes from the elevator doublet flight data. This was accomplished with the use of the MATLAB system identification toolbox. A least-squares estimation routine in the toolbox was used to find the second-order system that best matched the aircraft's short period mode at each flight static margin. Pilot elevator commands were used as the input into the system, and the pitch rate was the

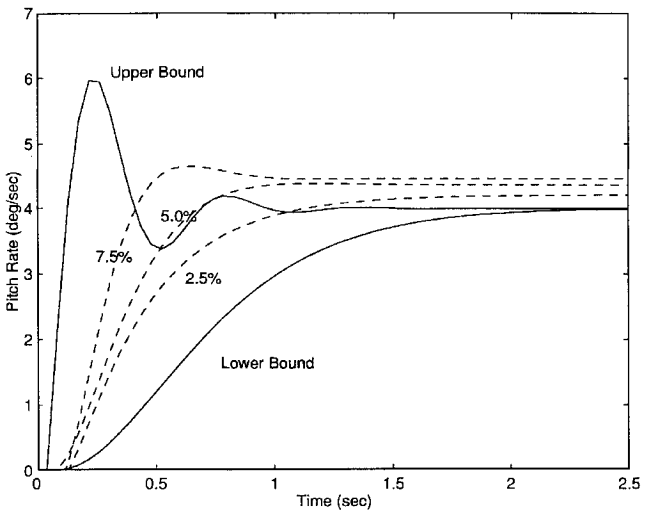

Fig. 16 Step responses of identified plants.

output. The step responses derived from this routine at the three static margins are shown along with the tracking bound step responses in Fig. 16. It can be seen in this plot that the damping ratios and natural frequencies of the identified systems are clearly within the tracking bounds and that the dc gains of the identified systems are close to the K_{pilot} value of 4 for a step elevator input. These dc gain results are within the error bounds in the MATLAB identification routine.[16]

Conclusion

Overall, the multi-input/multi-output QFT technique demonstrated its ability to work as designed for all of the controller designs. With the aid of a CAD package, the technique is a practical and very effective method for designing robust SASs. The flight test results from this design showed that the controller had met the required performance specifications over the entire flight envelope of a variable c.g. delta-wing UAV. The tracking performance of the vehicle appeared to be extremely close if not precisely within the desired tracking performance range for all static margins. In addition to meeting the desired performance specifications, the aircraft also demonstrated the ability to automatically retrim itself during c.g. shifts and in situations where the elevator trim angles were set erroneously. Finally, the pilot expressed comfort with the closed-loop aircraft handling qualities for a static margin range of 2.5–7.5% and a velocity range of 80–140 ft/s, as well as for an entire flight from takeoff to landing. The results from these flight tests, which are only the second series of QFT flight tests to be performed, are very encouraging and should spawn future QFT flight control system designs throughout the flight control industry.

Acknowledgments

This work was partially supported by Manned Flight Simulators, U.S. Naval Air Warfare Center, Patuxent River, Maryland, under Contract N60921-920D-A303. The authors would like to express their thanks to Steve Rassmussen and Constatine Houpis of Wright–Patterson Air Force Base in Dayton, Ohio. Without the technical documents, computer programs, and advice they provided, this research would not have been possible. The authors would also like to express their deepest thanks to all faculty and staff at NCSU who participated in the preparation, maintenance, and flight testing of the research vehicle. Finally, a special thanks goes to Justin Thomas, who provided the necessary system identification routines associated with this research.

References

[1]Horowitz, I. M., and Sidi, M., "Synthesis of Feedback Systems with Large Plant Ignorance for Prescribed Time Domain Tolerance," *International Journal of Control*, Vol. 16, No. 2, 1972, pp. 287–309.

[2]Horowitz, I. M., "A Synthesis Theory for Linear Time-Varying Feedback Systems with Plant Uncertainty," *IEEE Transactions*, AC-20, 1975, pp. 454–463.

[3]Horowitz, I. M., "Quantitative Synthesis of Uncertain Multiple Input-Output Feedback Systems," *International Journal of Control*, Vol. 30, No. 1, 1979, pp. 81–106.

[4]Yaniv, O., and Horowitz, I. M., "A Quantitative Design Method for MIMO Linear Feedback Systems Having Uncertain Plants," *International Journal of Control*, Vol. 43, No. 2, 1986, pp. 401–421.

[5]Houpis, C. H., "Quantitative Feedback Theory (QFT): Technique for Designing Multivariable Control Systems," Air Force Wright Aeronautical Lab., AFWAL-TR-86-3107, Wright–Patterson AFB, OH, Jan. 1987.

[6]D'Azzo, J. J., and Houpis, C. H., *Linear Control System Analysis and Design, Conventional and Modern*, 3rd ed., McGraw–Hill, New York, 1992, Chap. 21.

[7]Houpis, C. H., and Lamont, G. B., *Digital Control Systems: Theory, Hardware, Software*, 2nd ed., McGraw–Hill, New York, 1992.

[8]Bossert, D. E., et al., "Design of Discrete Robust Controllers Using Quantitative Feedback Theory and a Pseudo Continuos Time Approach," *Recent Developments in Quantitative Feedback Theory*, edited by Osita D. I. Nwokah, American Society of Mechanical Engineers, New York, 1990.

[9]Jayasuriya, S., "Benchmark Problem Solution by Quantitative Feedback Theory," *Journal of Guidance, Control, and Dynamics*, Vol. 15, No. 5, 1992, pp. 1087–1093.

[10]Nwokah, O., Jayasuriya, S., and Chiat, Y., "Parametric Robust Control by Quantitative Feedback Theory," *Proceedings of the American Control Conference*, Vol. 2, Inst. of Electrical and Electronics Engineers, Piscataway, NJ, 1991, pp. 1975–1980.

[11]Yang, J. S., "Controller Design for the F-14 Pitch Axis Control Problem Using the Quantitative Feedback Theory Approach," *Proceedings of the American Control Conference*, Vol. 2, Inst. of Electrical and Electronics Engineers, Piscataway, NJ, 1991, pp. 1995–2000.

[12]Bossert, D. E., "Design of Robust Quantitative Feedback Theory Controllers for Pitch Attitude Hold Systems," *Journal of Guidance, Control, and Dynamics*, Vol. 17, No. 1, 1992, pp. 217–219.

[13]Lacey, D. J., Horowitz, I. M., Houpis, C. H., and Sheldon, S. N., "A Robust Digital Flight Control System for an Unmanned Research Vehicle Using Quantitative Feedback Theory," *Quantitative Feedback Theory Symposium Proceedings*, U.S. Air Force Wright Lab., WL-TR-92-3063, Wright–Patterson AFB, OH, 1992, pp. 154–163.

[14]Fontenrose, P., "Design and Flight Testing of a Pitch Rate Stability Augmentation System via Quantitative Feedback Theory," M.S. Thesis, Dept. of Aerospace Engineering, North Carolina State Univ., Raleigh, NC, Dec. 1995.

[15]Perkins, J. N., Vess, R.J., and Hall, C. E., Jr., "Student Design, Construction, and Flight Testing of Stability Augmented RPV's," AIAA Paper 93-0422, Jan. 1993.

[16]Anon., "MATLAB User's Guide," Mathworks Inc., Natick, MA, Aug. 1992.

[17]Ashby, D., and Dudley, M., "Potential Flow Theory and Operation Guide for the Panel Code PMARC," NASA TM-102851, July 1991.

[18]Thomas, J. W., "Development of a MDAS System for Parameter Estimation of a UAV," M.S. Thesis, Dept. of Aerospace Engineering, North Carolina State Univ., Raleigh, NC, Dec. 1995.

[19]Fontenrose, P., and Thomas, J., "Design and Analysis of a Finite Impulse Response Controller for Stability Augmentation of a Relaxed Stability Remotely-Piloted Vehicle," *Proceedings of the AIAA Southeastern Regional Student Conference, Graduate Division* (Huntsville, AL), AIAA, Washington, DC, 1994.

[20]McLean, D., *Automatic Flight Control Systems*, Prentice–Hall, Englewood Cliffs, NJ, 1990, pp. 155–157.